Ink-jet printing of In2O3 /ZnO 2D-structures from solution

Jenny Jouin, Barbara Malič, Danjela Kuščer, Gregor Trefalt, Marija Kosec

journal of the American Ceramic Society
Incorporating Advanced Ceramic Materials and Communications

Ink-jet printing of In_2O_3/ZnO 2D-structures from solution

Journal:	*Journal of the American Ceramic Society*
Manuscript ID:	Draft
Manuscript Type:	Article
Date Submitted by the Author:	n/a
Complete List of Authors:	Tellier, Jenny; Jozef Stefan Institute, Electronic Ceramics Department Malic, Barbara; Jozef Stefan Institute, Electronic Ceramics Department Kuscer, Danjela; Jozef Stefan Institute, Electronic Ceramics Department Trefalt, Gregor; Jozef Stefan Institute, Electronic Ceramics Department Kosec, Maria; Jozef Stefan Institute, Electronic Ceramics Department
Keywords:	ink-jet, indium/indium compounds, thin films, printing, sol-gel

Ink-jet printing of In_2O_3/ZnO 2D-structures from solution

Jenny Tellier, Barbara Malic [*#], Danjela Kuscer, Gregor Trefalt and Marija Kosec[#]

Jožef Stefan Institute, Jamova 39, SI-1000 Ljubljana, Slovenia

Abstract

In_2O_3-ZnO 2D-structures were processed by ink jet printing and heating at temperature as low as 150°C with the aim for implementation in transparent flexible electronics. Such low temperatures would enable the use of polymeric substrates.

The In-Zn-solution precursor, based on In-alkoxide and Zn-acetate in 2-methoxyethanol, was originally designed for Chemical Solution Deposition of thin films. To adapt it for piezoelectric ink-jet printing, the viscosity and surface tension were adjusted by the addition of a more viscous 1,3-propanediol. The optimum values of 9.6 mPas and 34 mN/m were obtained for the ink consisting of 55 volume % of 1,3-propanediol. The printing parameters: the temperatures of the cartridge and the substrate, and the drop spacing were adjusted to allow patterning with a 40 μm resolution on SiO_x/Si and glass substrates.

The ink-jet printed 2D-structures heated at 150°C were organics-free, amorphous and upon heating at 450°C they crystallised without any preferential orientation, similarly as the spin-coated thin films, which were studied as reference.

1 Introduction

Many electronic /microelectronic devices are manufactured by depositing the material on a selected substrate via physical or chemical routes, followed by patterning in a desired

[*] Author to whom correspondence should be addressed: barbara.malic@ijs.si.
[#] Member, American Ceramic Society.
The work was supported by the Slovenian Research Agency program P2-0105 and the EU 6 FP project MULTIFLEXIOXIDES (NMP3-CT-2006-032231).

shape. Patterning is generally performed by various lithography techniques which consist of several processing steps including deposition of the resist, exposure, development, selective etching, and removal of the resist, resulting in a complex and costly process. For manufacturing low-cost electronics, simple, versatile and cost-efficient techniques are required. In contrast to subtractive lithographic approaches the additive or direct writing techniques, such as ink-jet printing [1, 2] enable patterning of structures on different substrates [3]. Ink-jet printing includes formation of small droplets of ink and their deposition on the substrate. The accurate drop-volume control and precise drop-positioning enable shaping of complex patterns [2] with a high resolution [4]. In this simple, low-waste, non-contact technique a selected pattern is built layer-by-layer. The printing information is created directly via computer and stored digitally and therefore enables easy modifications of device structure and architecture. In a piezoelectric-type ink-jet printer, the droplets are formed by mechanical compression of the ink through a nozzle. The ink consists of a material which is dispersed [5] or dissolved [6] in a solvent. It should have fixed ranges of viscosity and surface tension depending on the printer specifications in order to generate a proper stream of droplets [7, 8, 9]. Spreading of the ink on the substrate should be controlled to ensure a high resolution of the pattern [10].

Metal-oxides having the electronic configuration of $(n-1)d^{10}ns^0$ with $n\geq5$ attract a lot of interest for optical and electrical applications [11]. These transparent conductive oxides (TCOs) are characterized by a high optical transparency and a high electronic conductivity [11, 12]. They are used as transparent electrodes for flat-panel displays and solar cells [13, 14]. In thin-film-transistor (TFT) technology these oxides are used either as active channel layers or as source and drain electrodes [15, 16, 17]. Indium–zinc oxide (IZO) is characterised by a high mobility of charge carriers and a tunable conductivity [18]. An important advantage of IZO is the possibility to prepare amorphous thin films by physical vapor deposition at

room temperature [19, 20, 21]. Upon heating, the films crystallise as a mixture of In_2O_3 and ZnO [16, 22, 23, 24]. In contrast, ZnO thin films crystallise even when deposited at room temperature [24, 25]. It should be noted that amorphous films are characterised by a comparable mobility of charge carriers and a much lower roughness as compared to crystalline films as a consequence of absence of grain boundaries. [26].

TFT processing currently consists of IZO thin film deposition followed by patterning. A number of techniques have been investigated for many different compositions of IZO. Among physical methods sputtering seems to be the most widely used [16, 17, 20, 23, 24, 27, 28, 29]. Some reports on pulsed lased deposition [30], spray pyrolysis [31], reactive thermal oxidation [32], and reactive ion beam assisted evaporation [33] are also available.

Recently, chemical solution deposition (CSD) of inorganic thin films for TFT applications has been studied. The IZO films with the Zn/(In+Zn) molar ratio equal to 0.5 prepared from zinc acetate dihydrate and indium nitrate trihydrate in 2-methoxyethanol, with the addition of monoethanolamine, spin-coated and heated at 650°C, had a high optical transmittance of 80 to 85 % and a low resistivity of $1.5.10^{-3}$ Ω.cm. The films were crystalline with the average grain size of around 40 nm. [34]. ZnO thin films prepared from zinc-acetate dihydrate dissolved in 2-methoxyethanol by spin-coating and heating at 150°C in air were organics-free, amorphous, and crystallized upon heating to 450 °C. The films were transparent, with a transmission of over 80 % in the visible range. The resistivity of the 120 nm thick ZnO films processed at 150 °C was 57 MΩcm and upon heating at 450 °C it decreased to 1.9 kΩcm. [35].

Uniform and continuous IZO thin films have been processed by ink-jet printing and annealing at 600°C. The ink was based on zinc and indium halides in acetonitrile. [36]. ZnO thin films, printed with the ink based on zinc acetate dihydrate, ethylene glycol, ethanol and glycerine, crystallised upon heating at 500°C in air, however they were cracked [37].

The TFTs consisting of sputtered IZO source/drain electrodes and ink-jet printed Ga-In-Zn-O (GIZO) semiconductor were reported by Kim et al [38]. The precursor for ink-jet printing was based on zinc acetate, indium nitrate and gallium nitrate dissolved in 2-methoxyethanol, monoethanolamine and acetic acid. The GIZO layer was heated at 450°C. Poor characteristics of the TFT were explained as due to non-uniform film formation and imperfect contacts with other layers.

The aim of our study was to pattern organics-free, amorphous IZO 2D-structures with heating at temperatures not higher than 150°C. Although in our study silicon and glass substrates were employed, the ink was designed for the deposition on polymeric substrates. It should be noted that such substrates are prerequisite for low-cost, transparent and flexible electronics. The solution precursors, originally designed for CSD of IZO thin films by spin-coating, were modified in terms of viscosity and surface tension so that they could be used for ink-jet printing of continuous and patterned 2D structures on selected substrates. The printing parameters: the cartridge temperature, the substrate temperature and the drop spacing, were adapted accordingly. The printed 2D structures were characterized and compared with the CSD-derived thin films. The chemical composition, homogeneity and microstructure of the films and 2D structures prepared at 150°C and 450°C are discussed.

2 Experimental details

2.1 Processing

The solution for CSD of thin films, further referred as the CSD-solution, corresponded to the nominal film composition of 89.3 wt. % of In_2O_3 and 10.7 wt. % of ZnO, or to the molar ratio x=Zn/(In+Zn) of 0.2. It was prepared by dissolving indium (III) isopropoxide (99.9%, Alfa Aesar) in 2-methoxyethanol (2MOE) (99.3+%, Alfa Aesar). The mixture was stirred in a flask and kept at 40°C for two hours in dry nitrogen. Zinc acetate dihydrate (99%,

Fluka) was added in the flask and dissolved upon stirring at 40°C for two hours. The 0.25 M CSD-solution was cooled naturally, filtered and stored in a fridge. It was transparent, particle-free and stable for longer than one month.

The ink for ink-jet printing was prepared by mixing the CSD-solution with the solvent 1,3-propanediol (1,3-PD) at room temperature. The volume ratio of 1,3-PD : 2MOE was varied from 0:1 to 0.75:0.25. After preliminary experiments with the 0.25 M ink, the concentration of the ink was adjusted to 0.05 M in all cases.

The IZO thin films were prepared by depositing the CSD-solution on soda-lime glass and SiO_x/Si by spin coating at 3000 rpm for 30 s. Prior to the deposition, the substrates were cleaned with a mixture of ammonia, hydrogen peroxide and water in the volume ratio 1:1:6 at 50 °C, rinsed with distilled water and dried. After each deposition, the films were heated on a hot plate at 150°C for 1 hour in air. The coating and heating steps were repeated four times. Selected thin films were heated after each deposition on hot plates at 150°C for 10 minutes in air and additionally at 450°C for 30 minutes in air.

We used a piezoelectric ink-jet printer (Dimatix DMP2831) for printing experiments. To obtain continuous 2D structures with a good resolution, the temperature of the solution in the cartridge, the temperature of the substrate and the drop spacing were optimised. The structures were printed on soda-lime glass and on SiO_x/Si substrates, heated on a hot plate at 150°C for 1 hour in air, or at 150°C for 10 minutes and at 450°C for 30 minutes. The thickness of the deposits was measured by a profilometer (Taylor Hobson Form Talysurf).

2.2 Characterisation

The surface tension was measured by a stalagmometer and the dynamic viscosity by a rheometer (Anton Paar, RheolabQC) at room temperature. The viscosity results are given at a

shear rate of 1000 s^{-1}. The contact angles of the liquids on different substrates were measured by implementing the software ImageJ combined by the drop analysis plugin [39].

The precursor solution and the ink were dried at 100°C for 24h in air. The thermal decomposition of the as-dried xerogels was investigated by thermogravimetric and differential thermal analyss (TG/DTA, Netzsch STA 409) from room temperature to 650°C in flowing air (100 $mL.min^{-1}$), with a heating rate of 10 K/min, in Pt crucibles. The sample mass was about 50 mg in all cases.

The CSD-films and the printed structures on SiO_x/Si substrates were analysed by Fourier Transform Infra-Red (FTIR) spectroscopy (Perkin Elmer FTIR Spectrum 100, 4000 cm^{-1} to 600 cm^{-1}). The band positions including the base line correction were determined by the Spectrum program (Perkin Elmer). The films were further characterized by X-ray diffraction (XRD, PANalytical X'pert Pro diffractometer, $CuK_{\alpha 1}$ radiation). The data were collected in the 2θ–range from 20° to 65°, with a step of 0.034° and an exposure time of 200 s per step. The peak positions and the relative heights of the peaks were determined from the experimental patterns. The phases present were identified using the PDF-2 database [40].

The fracture surfaces of the films were also investigated by a Field Emission Scanning Electron Microscope (SEM Supra 35VP, Carl Zeiss) with an operating voltage of 5 kV.

The morphology of the films was analysed by the atomic force microscope (AFM Nanoscope IIIa, Digital Instruments). A V-shaped silicon nitride cantilever coated with gold was used for contact-mode imaging with a typical spring constant of 0.05 N/m, and a pyramidal tip. The base side of the tip was 4 µm long, its nominal radius was 10 nm, and the tip front angle measured 15°.

3 Results and discussion

3.1 Processing

The viscosity and the surface tension of the CSD-solution measured at room temperature were 3.4 mPas and 30 mN/m, respectively. The wetting angle of the CSD-solution on all substrates was too low to be measured. The CSD-solution was further spin coated on SiO_x/Si and glass substrates. The films were without any defects, and those deposited on glass substrates were transparent.

The target values of the viscosity and surface tension of the ink, proposed by the ink-jet printer producer, are 10 - 12 mPas and 28 - 32 mN/m, respectively [41]. Clearly, the viscosity of the CSD-solution needed to be adjusted for ink-jet printing. To increase the viscosity, the 1,3-PD with the viscosity of 41.5 mPas was admixed to the original CSD-solution. The viscosity and the surface tension of the liquid increased with increasing amount of 1,3-PD (Figure 1). The optimum viscosity of 9.6 mPas and surface tension of 34 mN/m were obtained for the mixture consisting of 55 vol % of 1,3-PD and 45 vol % 2MOE. After preliminary experiments, the metal concentration of the ink was reduced from the original 0.25 M to 0.05 M in order to reduce the thickness of a single layer and avoid cracking [37, 42]. The latter IZO ink was further used for printing experiments.

The contact angles of the IZO ink on glass and SiO_x/Si were 43° and 28° respectively. We therefore expected a better resolution of the printed structures on glass than on SiO_x/Si. Namely, lower contact angles should favour spreading of the ink across the substrate and result in a low resolution of the structure, while higher contact angles could result in a higher thickness and formation of cracks.

The thermal decomposition of the as-dried CSD-solution and ink were followed by thermal analysis. The TG/DTA curves are collected in Figure 2. The as-dried CSD-solution thermally decomposed upon heating to 650°C with a total weight loss of 29.9%. Between

200°C and 340°C the major weight loss of 15.1% was accompanied by a broad DTA exothermic peak at 290°C and a sharp one at 318°C. Weight losses in this temperature range were also observed in acetate-based precursors by Choi et al. [43]. The sample lost further 11% between 340°C and 550°C, the weight loss was accompanied by an exothermic DTA peak at 464 °C. We attributed these weight losses to the thermal decomposition of the residual organic groups present in the solution.

The total weight loss of the as-dried IZO ink upon heating to 650°C was 43.5%. Three steps of thermal decomposition could be distinguished. The first two steps of weight loss, 17.6% upon heating to 290°C and 10.2% between 290 °C and 340°C, resulted in a weight loss which was almost equivalent to the total weight loss of the CSD-sample. At 567°C a further weight loss of 15.7% was accompanied with a broad strong exothermic peak. This last effect was attributed to the presence of the 1,3-PD in the ink.

The CSD-solution was used for preliminary ink-jet printing experiments. We observed that at room temperature the solution jetted from the nozzles. The as-formed satellites did not recombine with the drops, which was detrimental for the resolution of the shape printed on SiO_x/Si substrate. The incorrect recombination of the satellite and the drop could be a consequence of a too low viscosity of the solution.

Further printing experiments were performed with the IZO ink with the adjusted viscosity and surface tension. However, at room temperature the ink was hardly ejected from the nozzle (Figure 3 left). Therefore the temperature of the cartridge was increased in order to decrease the viscosity and the surface tension of the ink. When the temperature reached 30°C, the ink jetted from the nozzle, forming a drop and a satellite which recombined (Figure 3 centre). At still higher temperatures, the ink jetted in random directions (Figure 3 right), which consequently resulted in a lower resolution of the structure. At the cartridge

temperature of 30°C and the voltage adjusted to 15 V spherical drops with a diameter of 25 µm were formed.

In addition to the temperature of the cartridge, the drop spacing had to be controlled to obtain continuous and well defined 2D structures. The drop spacing, defined as the distance between two drops on the substrate, characterized the quantity of the deposited material and thus the thickness of the deposited layer. The drop spacing of 10 µm resulted in a heavily cracked structure. The increase of the drop spacing to 20 µm yielded a continuous layer without any cracks. Further increase of the drop spacing to 30 µm resulted in a very thin and non-uniform deposit. A similar effect was observed when Cu suspension was ink-jet printed with a high drop spacing [44].

When the temperature of the substrate was kept at about 25 ^{o}C the ink merged in the centre of the deposit. In order to obtain a uniform deposit, the temperature of the substrate was increased to 60°C during printing. Increasing the substrate temperature enhanced the solvent evaporation from the printed deposit.

The optical micrograph of the surface of the 2D structure that was ink-jet printed on SiO_x/Si substrate, kept at the temperature of 60 °C, is shown in Figure 4. The edges of the structure were well defined. The aspect of the square was homogeneous, which means that its thickness was constant.

By using the optimised printing parameters, *i.e.* the cartridge temperature of 30°C, the substrate temperature of 60°C and the drop spacing of 20 µm, we printed a test pattern on SiO_x/Si. A detail of the structure is shown in Figure 5. The structure is uniform, with well defined edges without any fluctuations. The gap between two lines marked with an arrow is 40 µm wide which corresponds to the expected resolution specified for such type of ink-jet printer. The inset of Figure 6 includes a detail of the same pattern, printed on paper with the DMP black model fluid provided by Dimatix. The resolution of the two patterns was quite

similar. The same pattern was also printed on a glass substrate with a very good reproducibility. The 2D structure was uniform and transparent (Figure 6).

3.2 Phase composition and microstructure of the CSD-films and printed structures

The CSD-derived films and the printed 2D structures, deposited on SiO_x/Si substrate, and heated in air at 150°C and 450°C were analysed by FTIR spectroscopy to determine whether they contained organic residues. The infrared spectra of all specimens, collected in Figure 7, are very similar. The bands at 620 cm^{-1}, 800 cm^{-1}, 1015 cm^{-1} and 1149 cm^{-1} correspond to Si-O-Si bending and stretching modes, and obviously originate from the substrate [45]. We did not detect any characteristic bands of organic compounds [46, 47].

The XRD diagrams of the CSD-derived films and printed 2D-structures on SiO_x/Si substrates, heated at 150°C and at 450°C in air, are shown in Figure 8. The XRD patterns of both specimens heated at 150°C revealed only the diffraction peaks at 33° and 55°, originating from the substrate, and we therefore concluded that they did not have any long-range ordering. In the XRD diagrams of the CSD-derived film and printed 2D-structure, heated at 450°C, five broad peaks at 21.7 °, 30.8 °, 35.7 °, 51.4 ° and 61.0 ° were detected. These peaks correspond to the (211), (222), (400), (440) and (622) planes of polycrystalline cubic In_2O_3 (JCPDS card n°06-0416 [40]). We did not observe any preferential orientation. The DC magnetron sputtered IZO films on glass substrates crystallized with a strong (222) orientation when deposited on the substrate heated at 350°C or after annealing the amorphous specimens at 600°C [48]. About 10 nm thick IZO films on silicon substrates, prepared from zinc and indium acetates, and diethanolamine in 2-methoxyethanol, were amorphous upon heating at 500°C as confirmed by TEM [43].

The surface microstructure of the CSD-derived film on SiO_x/Si substrate, heated at 150°C in air, is shown in Figure 9. The topographic AFM image reveals a smooth film surface, with an image Rms roughness of 1.7 nm. The film thickness is about 190 nm.

The topographic AFM image of the printed 2D-structure heated at 150°C is shown in Figure 10. The image Rms of 9.5 nm is higher than that of the CSD-derived film, and attributed to a different deposition process.

The surface and the cross section images of the CSD-derived film on SiO_x/Si substrate, heated at 450°C in air, are shown in Figure 11. The image Rms roughness is 2.0 nm. This small increase of roughness upon heating is a consequence of the film crystallisation. The thickness of the film is about 185 nm, therefore almost no shrinkage occurred upon heating. The film contains a noticeable fraction of porosity and consists of fine grains with diameters between 20 and 50 nm. Lee et al. [34] prepared uniform, crack-free CSD-derived IZO films with the Zn/(Zn+In)=0.5 with grains of about 40 nm upon heating at 650°C.

The topographic AFM image and the cross-section SEM image of the printed 2D-structure on SiO_x/Si after heating at 450 ^oC are collected in Figure 12. The image Rms of 6.8 nm is higher than the values obtained for the CSD-film heated at 450°C, and is attributed to the effect of the selected deposition method. Due to the very hilly structure, the effect of crystallisation on the roughness is not evident. However the AFM image clearly shows the formation of small grains at 450°C. The thickness of the as-heated 2D-structure determined from the SEM image is about 35 nm, and the grain size in the range of 10-20 nanometres.

4 Summary

The precursor for Chemical Solution Deposition of thin films based on In-isopropoxide and Zn-acetate dihydrate in 2-methoxyethanol yielded defect-free transparent

films on glass substrates, but its viscosity of 3.4 mPas was much too low for ink-jet printing. By admixing a more viscous 1,3-propanediol to the CSD-solution in a 55 / 45 volume ratio, the appropriate values of viscosity and surface tension, 9.6 mPas and 34 mN/m, respecitvely, were obtained. After adjusting the printer cartridge temperature, drop spacing and substrate temperature the ink was succesfully printed with a 40 μm resolution on silicon and glass substrates.

The printed structures were transparent, amorphous and organics-free upon heating at 150 °C. They crystallize upon further hetaing at 450°C. Printing of the solution-derived ink was therefore a suitable method for patterning of 2D-structures on temperature-sensitive substrates, such as polymers.

Acknowledgments

The authors wish to thank Jena Cilensek, Silvo Drnovsek and Miha Skarabot for their support concerning thermal analyses, profilometry and atomic force microscopy. Petra Forte Tavcar from the Faculty of Natural Sciences and Engineering, University of Ljubljana, is acknowledged for the use of viscosimeter.

[1] M. Mott and J.R.G. Evans, "Zirconia/alumina functionally graded material made by ceramic ink jet printing", *Mater. Sci. Eng.*, A271, 344–352 (1999).

[2] S.B. Fuller, E.J. Wilhelm, and J.M. Jacobson, "Ink-jet printed nanoparticle microelectromechanical systems", *J. Microelectromech. Syst.*, 11 [1] 54-60 (2002).

[3] A. Pique and D.B. Chrisey, "Direct-write technologies for rapid prototyping applications: Sensors, electronics, and integrated power sources". San Diego, San Francisco, New York, Boston, London, Sydney, Tokyo, Academic Press (2002).

[4] K. Murata, J. Matsumoto, A. Tezuka, Y. Matsuba and H. Yokoyama, "Super-fine ink-jet printing: toward the minimal manufacturing system", *Microsyst. Technol.*, 12, 2-7 (2005).

[5] X. Ding, Y. Li, D. Wang and Q. Yin, "Fabrication of $BaTiO_3$ Dielectric Films by Direct Ink-Jet Printing", *Ceram. Int.*,30, 1885–1887 (2004).

[6] X. Ding, Y. Li, D. Wang and Q. Yin, "Preparation of $(Ba_xSr_{1-x})TiO_3$ sols for ceramic film jet-printing", *Mater. Sci. Eng.*, B99, 502-505 (2003).

[7] D. Heon Lee and B. Derby, "Preparation of PZT suspensions for direct ink jet printing", *J. Eur. Ceram. Soc.*, 24, 1069-1072 (2004).

[8] R. Noguera, M. Lejeune and T. Chartier, "3D fine scale ceramic components formed by ink-jet prototyping process", *J. Eur. Ceram. Soc.*, 25, 2055-2059 (2005).

[9] A. Pique, D.B. Chrisey and F.C.Krebs, "Fabrication and processing of polymer solar cells: A review of printing and coating techniques", *Sol. Energy mater.*, 93 (4) 394-412 (2009).

[10] E. Kunnari, J. Valkama, M. Keskinen and P. Mansikkamaki, "Environmental evaluation of new technology: printed electronics case study", *J Cleaner Prod.*, 17 [9] 791-799 (2009).

[11] H. Hosono, "Recent progress in transparent oxide semiconductors: Materials and device application", *Thin Solid Films*, 515, 6000-6014 (2007).

[12] T. Kamiya and H. Hosono, "Electronic Structures and Device Applications of Transparent Oxide Semiconductors: What Is the Real Merit of Oxide Semiconductors?", *Appl. Ceram. Techn.*, 2, 285-294 (2005).

[13] J.F. Wager, D.A. Keszler and R.E. Presley, "Transparent electronics", Springer, New York (2008).

[14] R.L. Hoffman, B.J. Norris and J.F. Wager, "ZnO-based transparent thin-film transistors", *Appl. Phys. Letters*, 82 [5], 733-735 (2003).

[15] P. Barquinha, A. Pimentel, A. Marques, L. Pereira, R. Martins and E. Fortunato, "Influence of the semiconductor thickness on the electrical properties of transparent TFTs based on indium zinc oxide", *J. Non-Cryst. Solids*, 352, 1749-1752 (2006).

[16] D.C. Paine, B. Yaglioglu, Z. Beiley, and S. Lee, "Amorphous IZO-based transparent thin film transistors", *Thin Solid Films*, 516 [17], 5894-5898 (2008).

[17] B. Yaglioglu, H. Yeom, R. Beresford and D. Paine, "High-mobility amorphous In_2O_3–10 wt% ZnO thin film transistors", *Appl. Phys. Lett.*, 89, 062103 3pp. (2006).

[18] G. Gonçalves, P. Barquinha, L. Raniero, R. Martins, and E. Fortunato, "Crystallization of amorphous indium zinc oxide thin films produced by radio-frequency magnetron sputtering", *Thin Solid Films* 516 [7], 1374-1376 (2008).

[19] T. Moriga, K. Shimomura, D. Takada, H. Suketa, K. Takita, K.I. Murai, and K. Tominaga, "In_2O_3-ZnO transparent conductive oxide film deposition on polycarbonate substrates", *Vacuum*, 83 [3], 557-560 (2008).

[20] R. Martins, P. Almeida, P. Barquinha, L. Pereira, A. Pimentel, I. Ferreira, and E. Fortunato, "Electron transport and optical characteristics in amorphous indium zinc oxide films", *J. Non-Cryst. Solids*, 352 [9-20 SPEC. ISS.], 1471-1474 (2006).

[21] W. Lim, Y.L. Wang, F. Ren, D.P. Norton, I.I. Kravchenko, J.M. Zavada, and S.J. Pearton, "Indium zinc oxide thin films deposited by sputtering at room temperature", *Appl. Surf. Science*, 254 [9], 2878-2881 (2008).

[22] N.L. Dehuff, E.S. Kettenring, D. Hong, H.Q. Chiang, J.F. Wager, R.L. Hoffman, C. H. Park, and D.A. Keszler, "Transparent thin-film transistors with zinc indium oxide channel layer", *J. Appl. Phys.* 97 [6], 064505 5pp. (2005).

[23] D.Y. Ku, I.H. Kim, I. Lee, K.S. Lee, T.S. Lee, J.H. Jeong, B. Cheong, Y.J. Baik, and W.M. Kim, "Structural and electrical properties of sputtered indium-zinc oxide thin films", *Thin Solid Films*, 515 [4], 1364-1369 (2006).

[24] T. Moriga, T. Okamoto, K. Hiruta, A. Fujiwara, I. Nakabayashi, and K. Tominaga, "Structures and physical properties of films deposited by simultaneous DC sputtering of ZnO and In_2O_3 or ITO targets", *J. Solid State Chem.*, 155 [2], 312-319 (2000).

[25] E. Fortunato, A. Pimentel, L. Pereira, A. Gonçalves, G. Lavareda, H. Aguas, I. Ferreira, C.N. Carvalho, and R. Martins, "High field-effect mobility zinc oxide thin film transistors produced at room temperature", *J. Non-Cryst. Solids*, 338–340, 806-809 (2004).

[26] A. J. Leenheer, J. D. Perkins, M. F. A. M. van Hest, J. J. Berry, R. P. O'Hayre and D. S. Ginley, "General mobility and carrier concentration relationship in transparent amorphous indium zinc oxide films", *Phys.Rev B* 77, 115215, 5pp., (2008).

[27] E. Fortunato, A. Pimentel, A. Gonçalves, A. Marques and R. Martins, "High mobility amorphous/nanocrystalline indium zinc oxide deposited at room temperature", *Thin Solid Films*, 502 [1-2], 104-107 (2006).

[28] P. Barquinha, G. Gonçalves, L. Pereira, R. Martins and E. Fortunato, "Effect of annealing temperature on the properties of IZO films and IZO based transparent TFTs", *Thin Solid Films*, 515 [24 SPEC. ISS.], 8450-8454 (2007).

[29] K.J. Saji and M.K. Jayaraj, "Optical and electrical properties of co-sputtered amorphous transparent conducting zinc indium tin oxide thin films", *Thin Solid Films*, 516, 6002-6007 (2008).

[30] N. Naghavi, A. Rougier, C. Marcel, C. Guéry, J.B. Leriche and J.M. Tarascon, "Characterization of indium zinc oxide thin films prepared by pulsed laser deposition using a $Zn_3In_2O_6$ target", *Thin Solid Films*, 360 [1-2], 233-240 (2000).

[31] M.M. Bagheri-Mohagheghi and M. Shokooh-Saremi, "The effect of high acceptor dopant concentration of Zn^{2+} on electrical, optical and structural properties of the In_2O_3 transparent conducting thin films", *Semicond. Sci. Technol.*, 18 [2], 97-103 (2003).

[32] T.C. Chen, T.P. Maand R.C. Barker, "Infrared transparent and electrically conductive thin film of In_2O_3", *Appl. Phys. Lett.*, 43 [10] 901-903 (1983).

[33] Y. Vygranenko, K. Wang, R. Chaji, M. Vieira, J. Robertson and A. Nathan, "Stability of indium-oxide thin-film transistors by reactive ion beam assisted deposition", *Thin Solid Films*, 517 [23], 6341-6344 (2009).

[34] S.Y. Lee, and B.O. Park, "Electrical and optical properties of In_2O_3-ZnO thin films prepared by sol-gel method", *Thin Solid Films*, 484 [1-2], 184-187 (2005).

[35] J. Tellier, D. Kuscer, B. Malic, J. Cilensek, M. Skarabot, J. Kovac, G. Gonçalves, I. Musevic and M. Kosec, "Transparent, Amorphous and Organics-Free ZnO Thin Films Produced by Chemical Solution Deposition at 150°C", *Thin Solid Films*, in press (2010), doi:10.1016/j.tsf.2010.03.010.

[36] D.H. Lee, Y.J. Chang, G.S. Herman and C.H. Chang, "A general route to printable high-mobility transparent amorphous oxide semiconductors", *Adv. Mater.*, 19, 843-847 (2007).

[37] W. Shen, Y. Zhao and C. Zhang, "The preparation of ZnO based gas-sensing thin films by ink-jet printing method", *Thin Solid Films*, 483, 382-387 (2005).

[38] Kim, G.H., Kim, H.S., Shin, H.S., Ahn, B.D., Kim, K.H. and Kim, H.J., "Inkjet-printed InGaZnO thin film transistor", *Thin solid films*, 517, 4007-4010 (2009).

[39] A.F. Stalder, G. Kulik, D. Sage, L. Barbieri, P. Hoffmann, "A snake-based approach to accurate determination of both contact points and contact angles", *Colloids Surf. A*, 286 [1-3], 92-103 (2006).

[40] PDF-ICDD, PCPDFW in Version 2.2, June 2001, International Centre for Diffraction Data (2002).

[41] www.dimatix.com

[42] L. Shapiro, S. Marx and D. Mandler, "Preparation and characterization of ultra-thin sol-gel films", *Thin Solid Films*, 515, 4624-4628 (2007).

[43] C.G. Choi, S.J. Seo and B.S. Bae, "Solution-processed indium-zinc oxide transparent thin-film transistors", *Electrochem. Solid-State Lett.*, 11 [1] H7-H9 (2008).

[44] B.K. Park, D. Kim, S. Jeong, J. Moon and J.S. Kim, "Direct writing of copper conductive patterns by ink-jet printing", *Thin Solid Films*, 515, 7706-7711 (2007).

[45] V.P. Tolstoy, I.V. Chernychova, and V. A. Skryshevsky, "Handbook of infrared spectroscopy of ultrathin films", John Wiley & sons (2003).

[46] S. Bandyopadhyay, G.K, Paul, R.Roy, S.K. Sen and S.Sen, "Study of structural and electrical properties of grain-boundary modified ZnO films prepared by sol-gel technique", *Mater. Chem. Phys.*, 74, 83-91 (2002).

[47] A. E. Jimenez-Gonzales, J.A. Soto Urueta and R. Suarez-Parra, "Optical and electrical characteristics of aluminum-doped ZnO thin films prepared by solgel technique", *J. Cryst. Growth*, 192, 430-438 (1998).

[48] Y.S. Jung, J.Y. Seo, D.W. Lee and D.Y. Jeon, "Influence of DC magnetron sputtering parameters on the properties of amorphous indium zinc oxide thin film", *Thin Solid Films*, 445, 63-71 (2003).

Figure captions

Figure 1: Viscosity (a) and surface tension (b) of the IZO solutions prepared with different 1,3-PD:2MOE volume ratios. The dotted lines indicate the optimum ranges of both quantities.

Figure 2: Thermogravimetric and differential thermal analyses (TG/DTA) of the as-dried a) CSD-solution and b) ink.

Figure 3: Image capture of the drop ejection of the IZO ink with the 1,3-PD:2MOE volume ratio of 55:45. The temperature of the cartridge ranged from 25°C to 35°C. The voltage was adjusted to obtain ejection of the drops from the nozzles.

Figure 4: A 2D structure of IZO printed with a drop spacing of 20 µm and a substrate temperature of 60°C. The temperature of the cartridge and ejection voltage were 30°C and 15 V, respectively.

Figure 5: Optical micrograph of a detail of the as-printed 2D structure on SiO_x/Si. Inset: a part of the same pattern printed on paper with the DMP black model fluid.

Figure 6: Optical micrograph of a detail of the as-printed 2D structure on glass substrate.

Figure 7: FTIR spectra of the CSD-derived films ink-jet printed 2D structures deposited on SiO_x/Si substrates, heated at 150°C and 450°C in air. The spectrum of the substrate is added as a reference.

Figure 8: Diffractograms of CSD-derived IZO films and printed structures on SiO_x/Si substrates heated at 150°C and at 450°C in air.

Figure 9: Topografic AFM image of the CSD-derived IZO film on SiO_x/Si, heated at 150°C in air.

Figure 10: Topografic AFM image of the printed 2D-structure on SiO_x/Si, heated at 150°C in air.

Figure 11: Topographic AFM image (a) and fracture-surface SEM (b) of the CSD-derived IZO film on SiO_x/Si, heated at 450°C in air.

Figure 12: Topographic AFM image (a) and fracture-surface SEM (b) of the printed 2D-structure on SiO_x/Si, heated at 450°C in air.

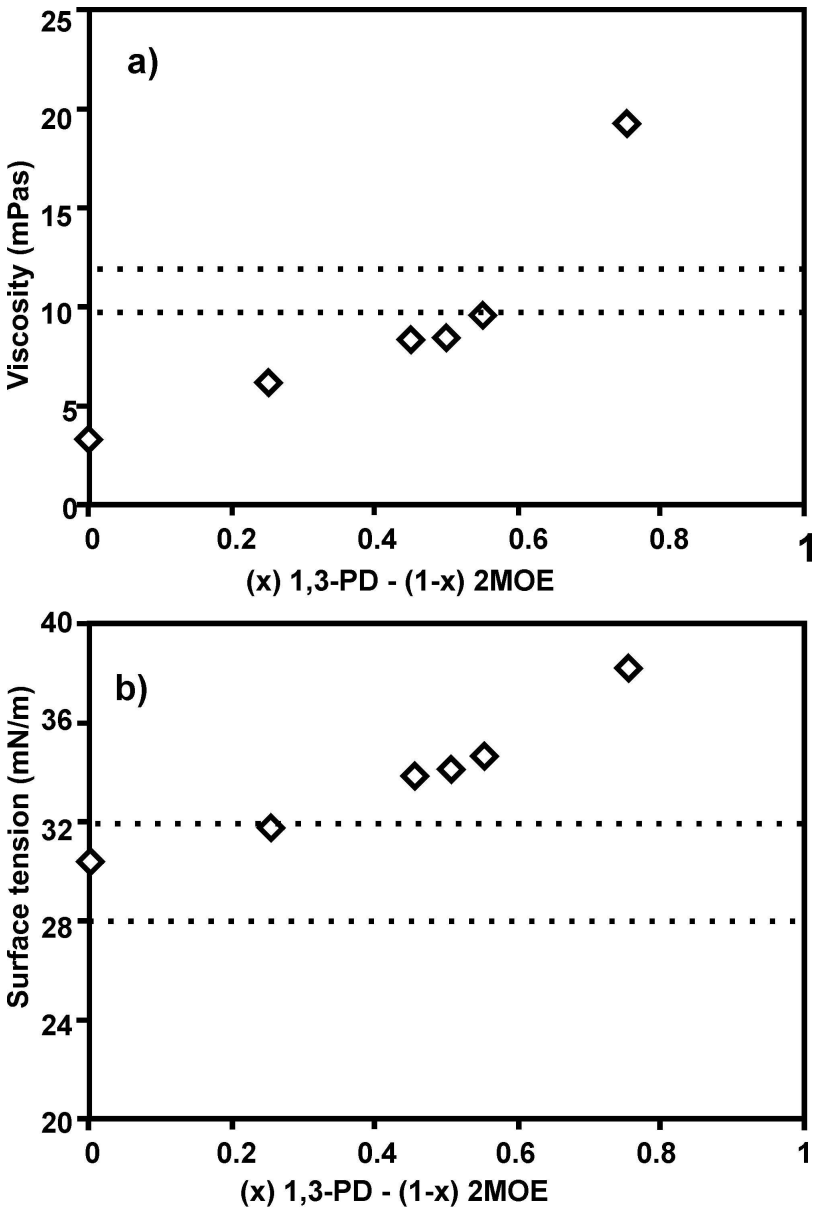

Figure 1: Viscosity (a) and surface tension (b) of the IZO solutions prepared with different 1,3-PD:2MOE volume ratios. The dotted lines indicate the optimum ranges of both quantities.

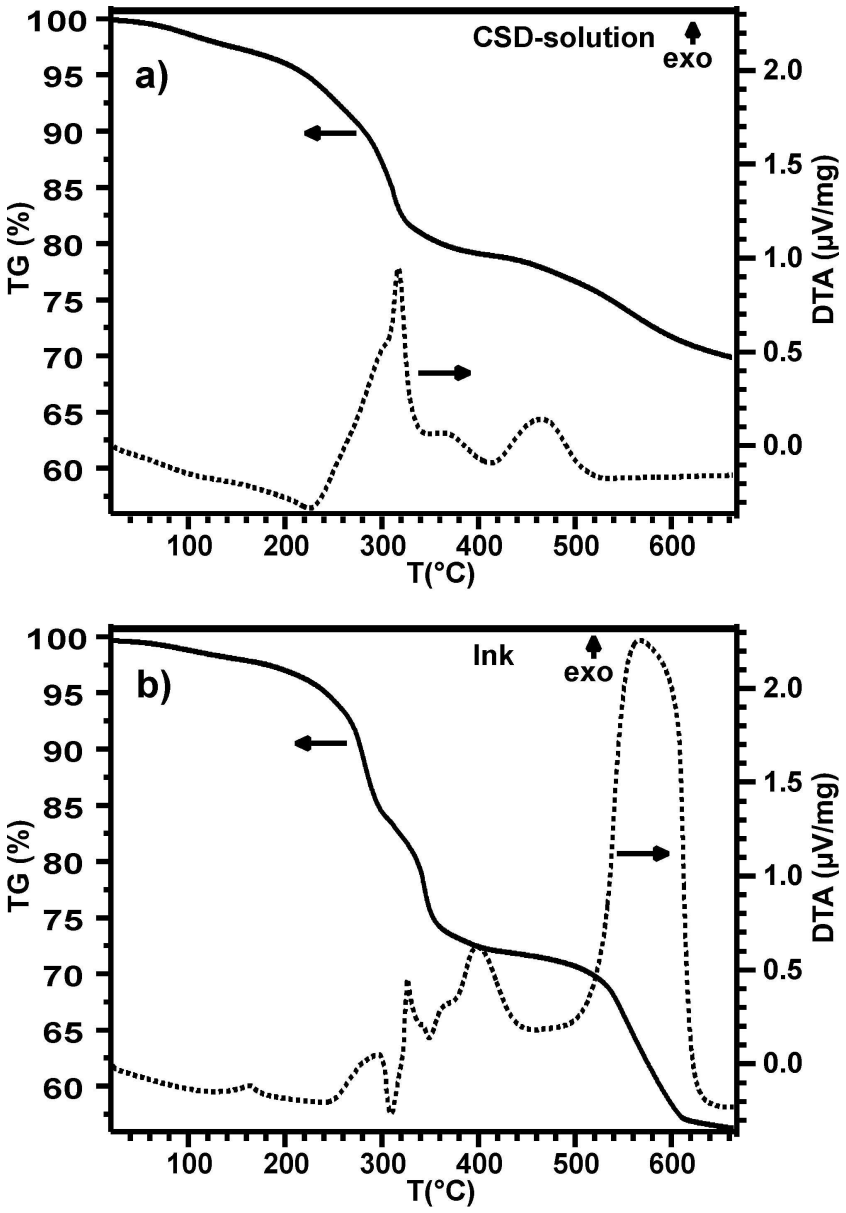

Figure 2: Thermogravimetric and differential thermal analyses (TG/DTA) of the as-dried a) CSD-solution and b) ink.

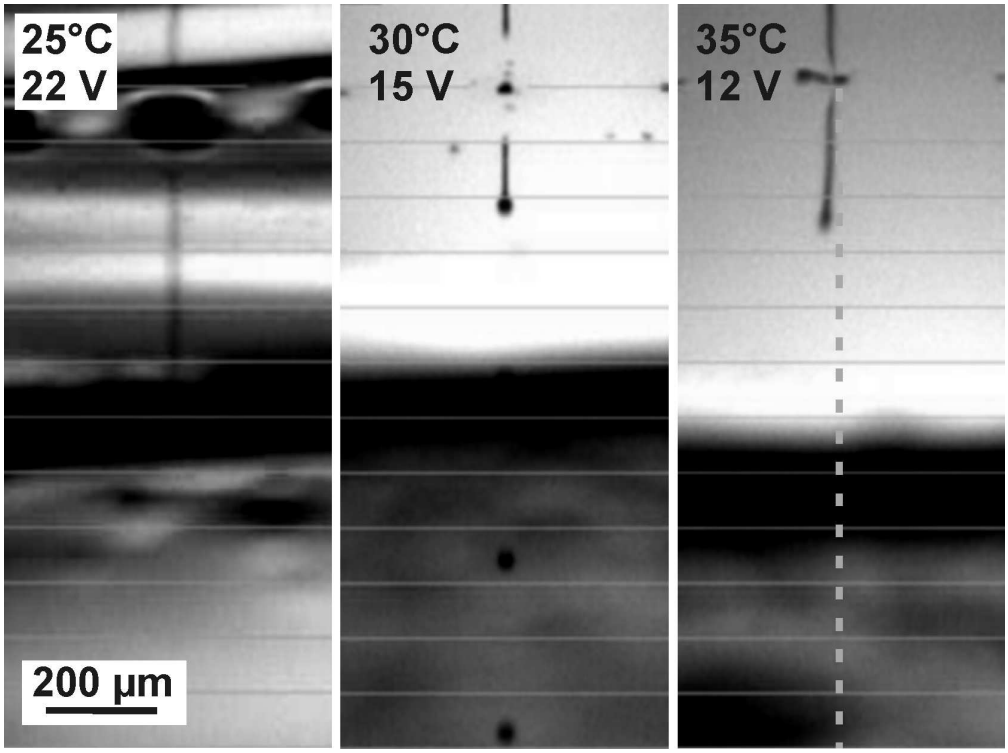

Figure 3: Image capture of the drop ejection of the IZO ink with the 1,3-PD:2MOE volume ratio of 55:45. The temperature of the cartridge ranged from 25°C to 35°C. The voltage was adjusted to obtain ejection of the drops from the nozzles.

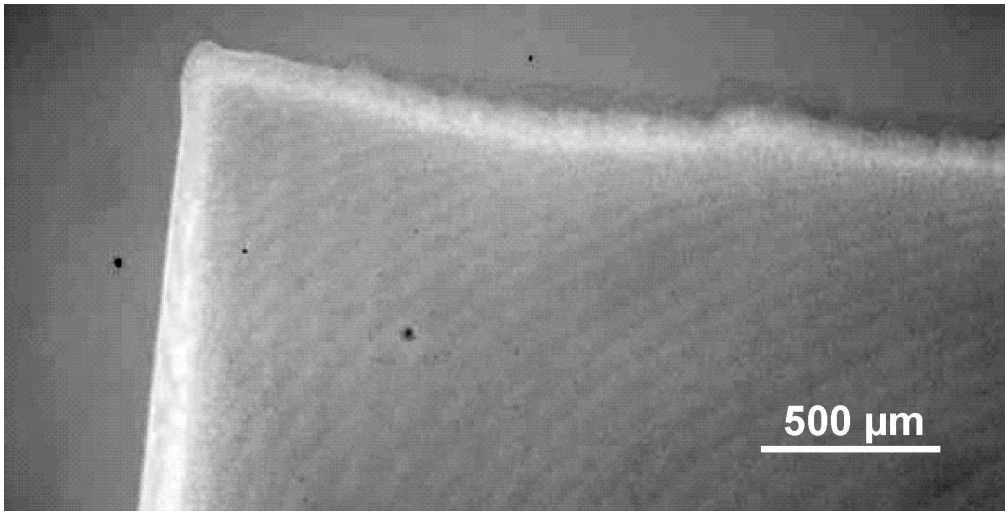

Figure 4: A 2D structure of IZO printed with a drop spacing of 20 µm and a substrate temperature of 60°C. The temperature of the cartridge and ejection voltage were 30°C and 15 V, respectively.

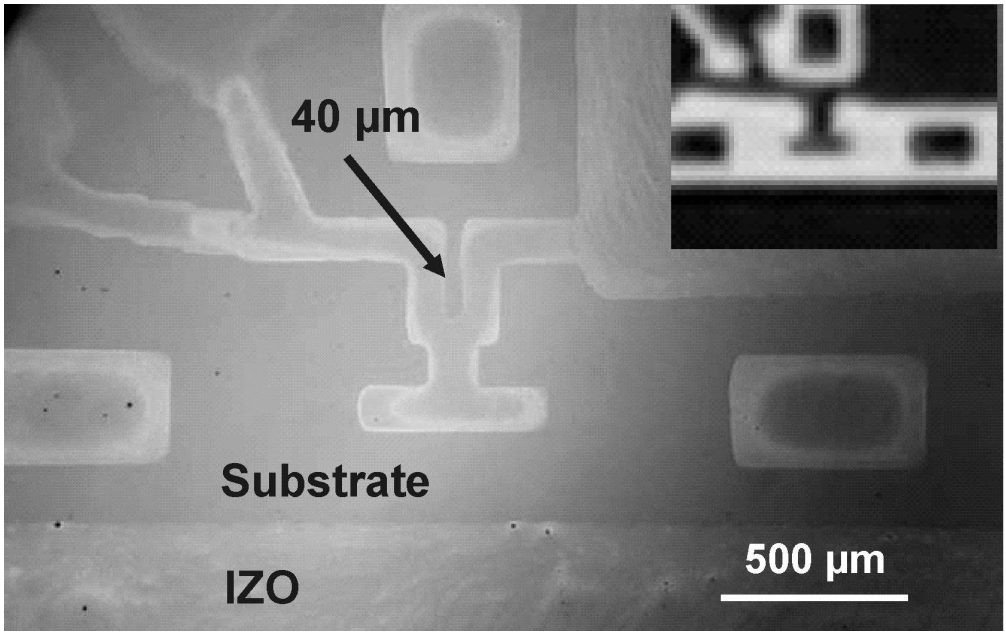

Figure 5: Optical micrograph of a detail of the as-printed 2D structure on SiO_x/Si. Inset: a part of the same pattern printed on paper with the DMP black model fluid.

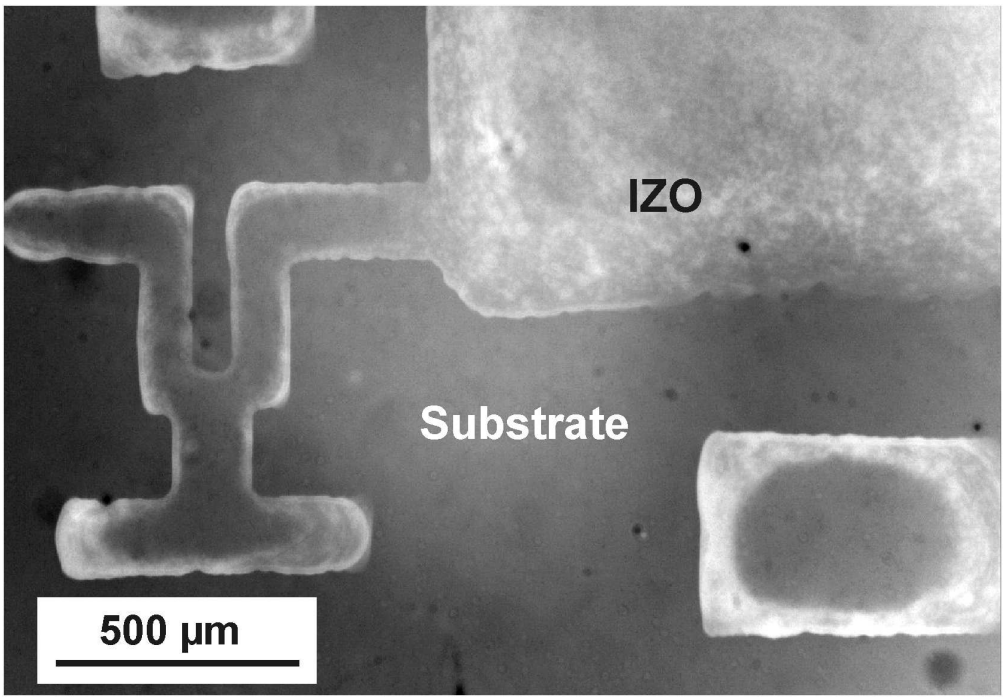

Figure 6: Optical micrograph of a detail of the as-printed 2D structure on glass substrate.

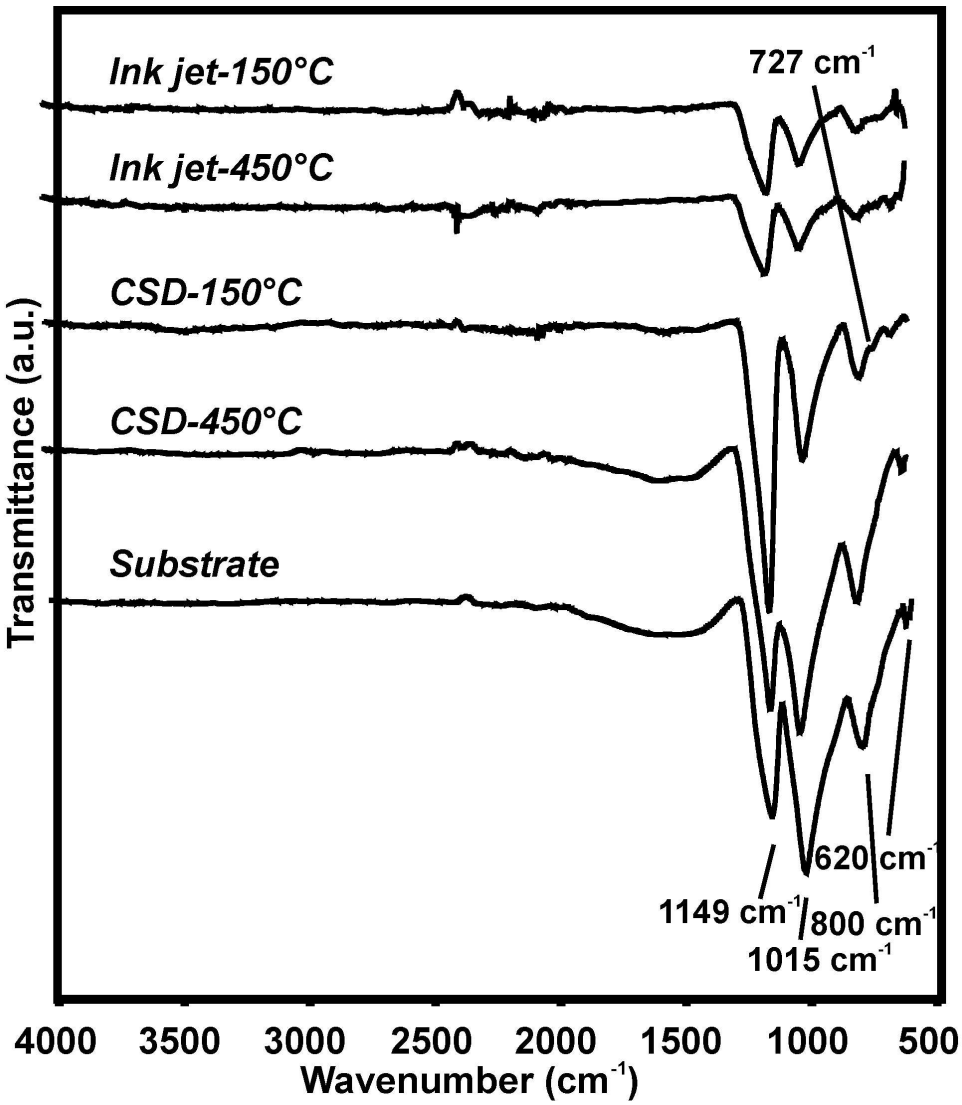

Figure 7: FTIR spectra of the CSD-derived films ink-jet printed 2D structures deposited on SiO_x/Si substrates, heated at 150°C and 450°C in air. The spectrum of the substrate is added as a reference.

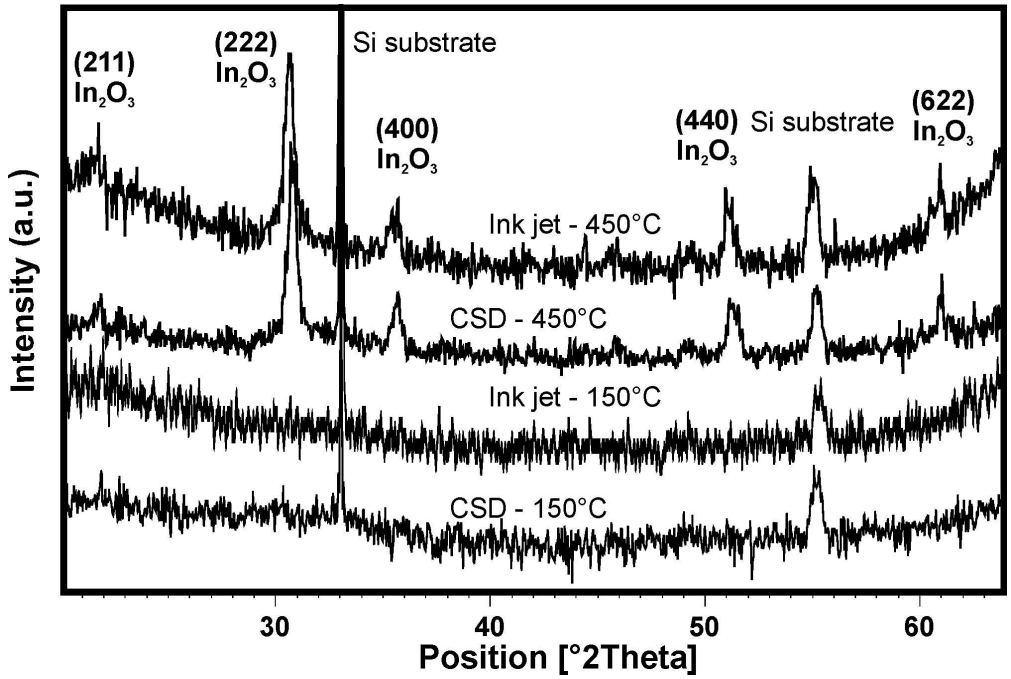

Figure 8: Diffractograms of CSD-derived IZO films and printed structures on SiO_x/Si substrates heated at 150°C and at 450°C in air.

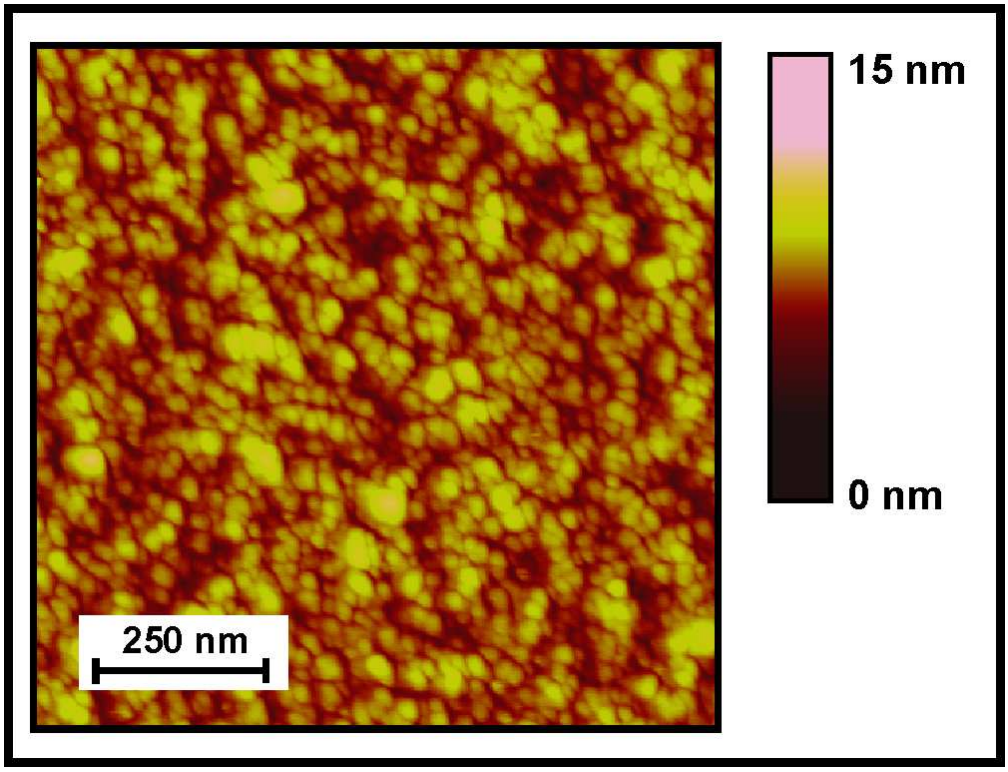

Figure 9: Topografic AFM image of the CSD-derived IZO film on SiO_x/Si, heated at 150°C in air.

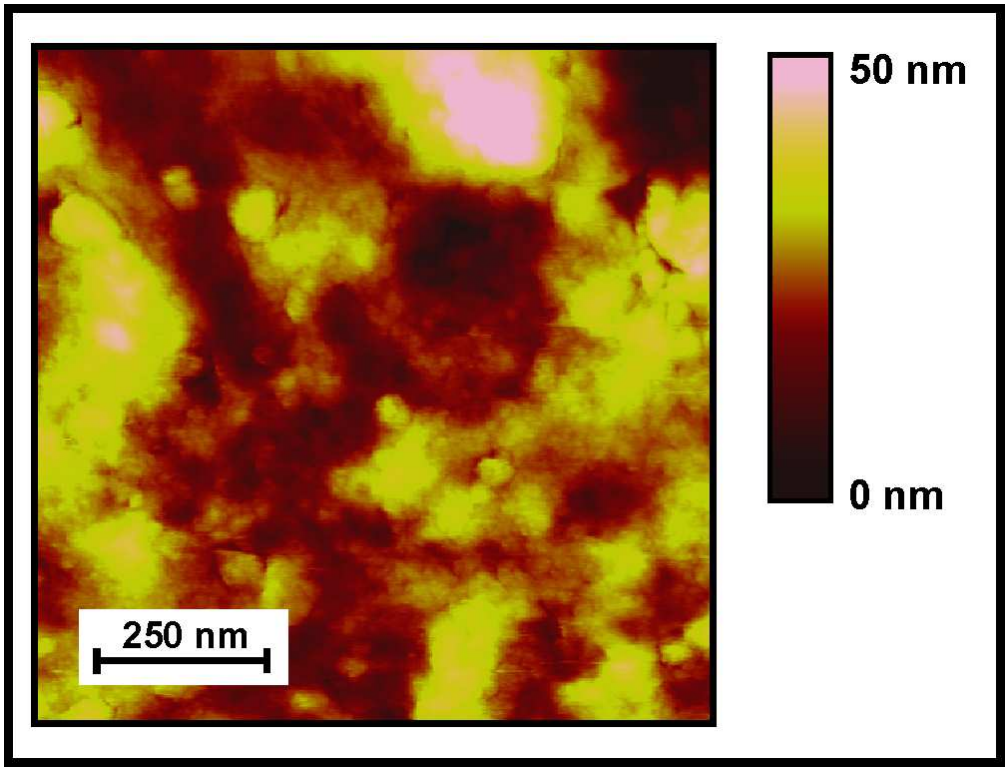

Figure 10: Topografic AFM image of the printed 2D-structure on SiO_x/Si, heated at 150°C in air.

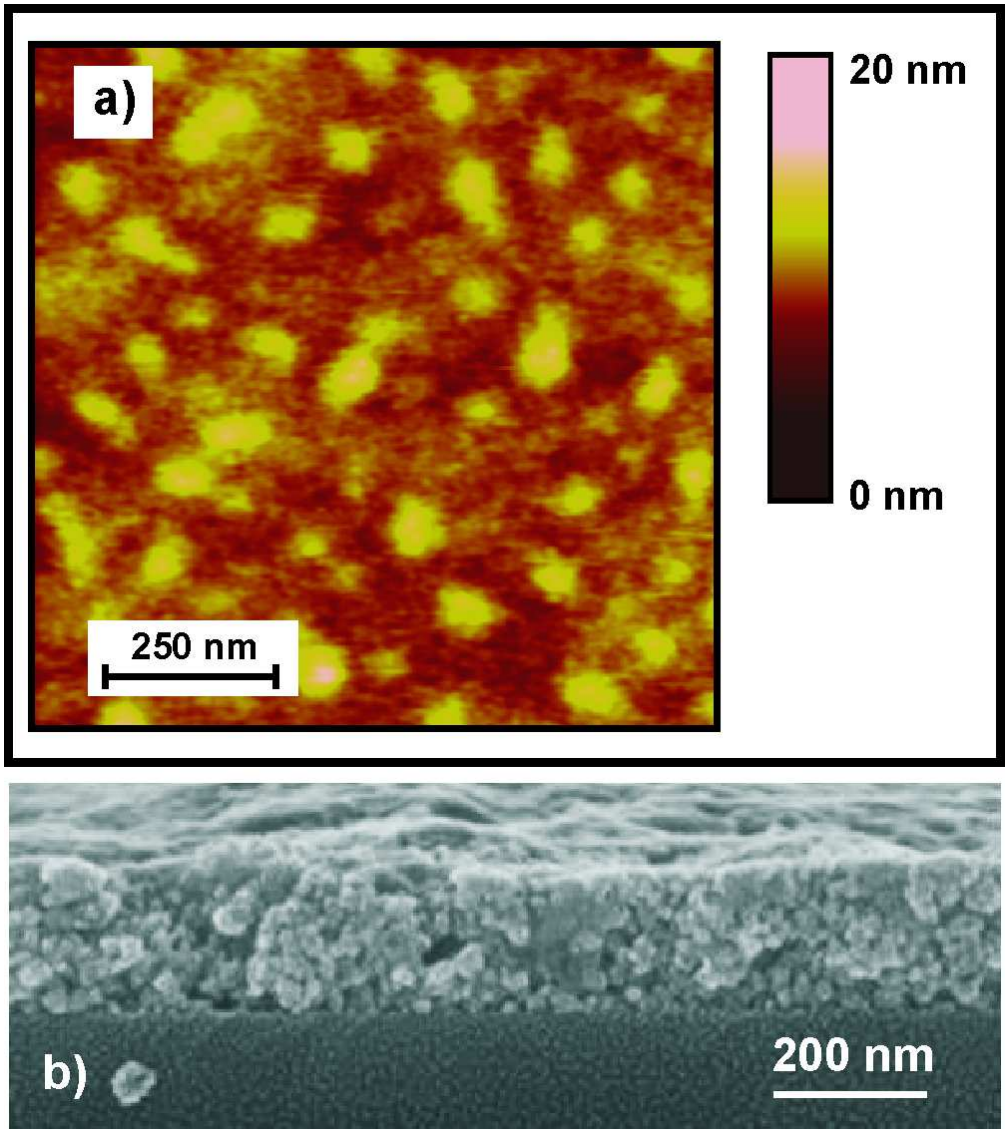

Figure 11: Topographic AFM image (a) and fracture-surface SEM (b) of the CSD-derived IZO film on SiO_x/Si, heated at 450°C in air.

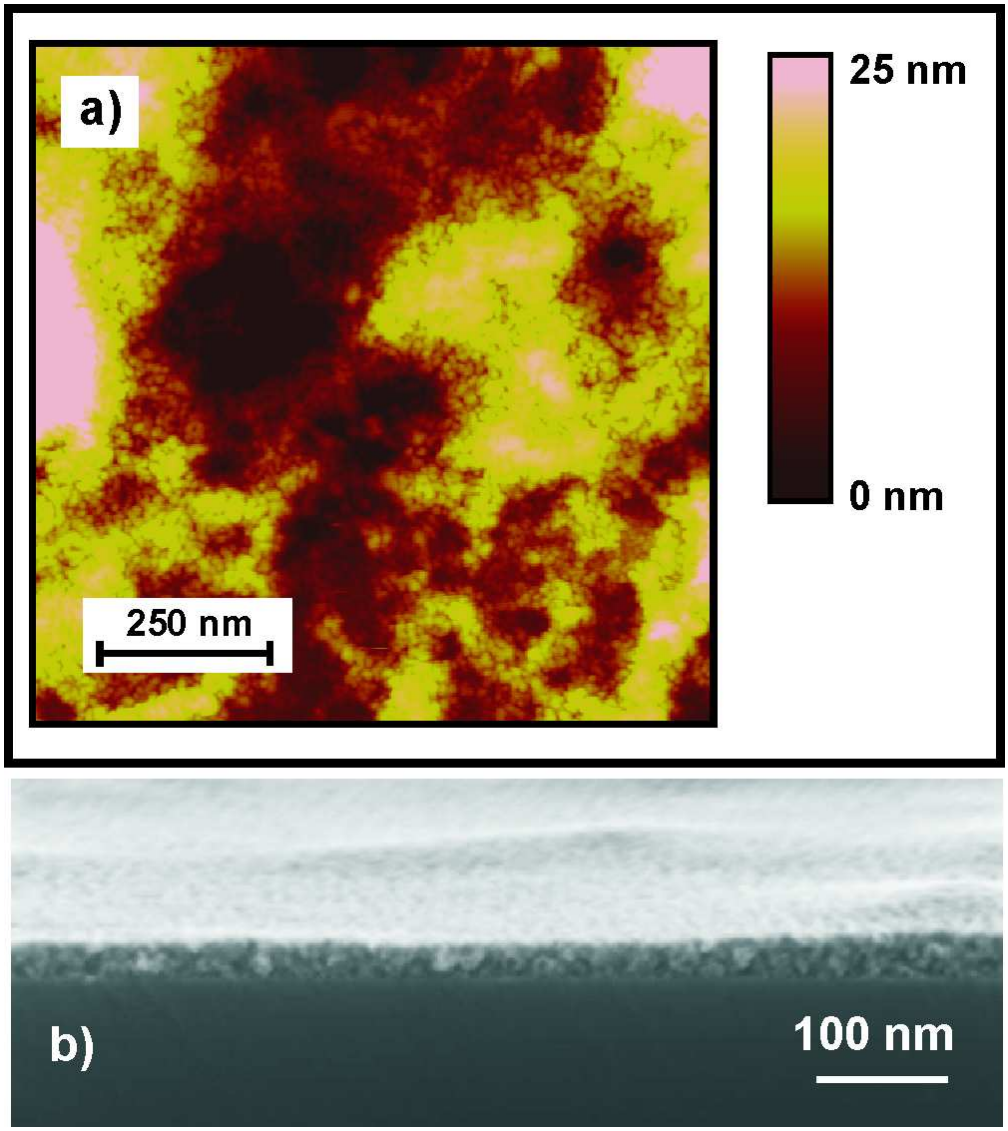

Figure 12: Topographic AFM image (a) and fracture-surface SEM (b) of the printed 2D-structure on SiO_x/Si, heated at 450°C in air.